atmosphere

Article

Assessment of Satellite Precipitation Products and Bias Correction Methods Over the Western Part of Saudi Arabia

Ibrahim H. Elsebaie, Atef Q. Kawara*, Ali O. Alnahit, and Raied Alharbi

Civil Engineering Department, King Saud University, P.O. Box 800, Riyadh 11421, Saudi Arabia; elsebaie@ksu.edu.sa (I.H.E.); 439106883@student.ksu.edu.sa (A.Q.K); alialnaheet@ksu.edu.sa (A.O.A.); rsalharbi@ksu.edu.sa (R.S.A).

* Correspondence: 439106883@student.ksu.edu.sa

Academic Editor: Firstname Lastname

Received: date
Revised: date
Accepted: date
Published: date

Citation: To be added by editorial staff during production.

Abstract: The limitation in the possibility of dealing with precipitation data sources with appropriate spatial-temporal distribution is a significant challenge in different parts of the world. Satellite-based precipitation (SBP) is becoming a dependable method for obtaining highly detailed rainfall estimates worldwide. However, the uncertainty associated with SBP remains significant and cannot be used without proper assessment, frequently requiring bias correction. In this study, the effectiveness of five different SBP methods (GPM, GPCP, CHIRPS, PERSIANN-CDR, and PERSIANN) in accurately replicating observed monthly rainfall was evaluated at 28 stations located in the western region of Saudi Arabia.   The most performed products were corrected using different bias correction methods. After conducting the analysis, it was found that the GPM product had the highest correlation coefficient of 0.56 and the lowest RMSE and MAE values among other products. As a result, GPM was the best of the other SBPs. Regarding the best bias correction method, the Artificial Neural Network (ANN) was more effective than traditional bias correction methods, including linear scaling, nonlinear, and quantile mapping methods. The average correlation coefficient before bias correction for GPM, GPCP, CHIRPS, PERSIANN-CDR, and PERSIANN on a monthly basis was 0.52, 0.4, 0.2, 0.43, and 0.26, respectively. This study asserts that the GPM may be deemed a dependable source of precipitation data for hydrological studies in the western region of Saudi Arabia.

Keywords: Precipitation products, ANN, GPM,Makkah, Saudi Arabia.

1. Introduction

Precipitation is an important factor in the water and energy cycles, with significant implications for hydrometeorology, agriculture, and water supply [1–4]. However, it is difficult to get dependable and enduring global precipitation data that has both high spatial and temporal resolutions [5–8]. While ground rain gauges can provide high temporal frequency precipitation information, the uneven distribution and scarcity of rain gauge networks limit their accuracy [9–12]. Thus, satellites have emerged as a viable option for monitoring precipitation on a regional or global level, offering a high level of accuracy in both temporal and spatial dimensions [13–15].

Several studies have compared ground gauges and satellite products, and many correction approaches have been proposed [16,17]. Satellite products have become famous since they give more spatial coverage and temporal resolution than ground rain gauges [18,19]. Several satellite precipitation products have been created internationally. There are five commonly utilized open-sourced satellite products: GPCP (Global Precipitation

Climatology Project), PERSIANN-CDR (Precipitation Estimation from Remotely Sensed Information using Artificial Neural Networks-Climate Data Record) , GPM (Global Precipitation Measurement), PERSIANN (Precipitation Estimation from Remotely Sensed Information using Artificial Neural Networks) and CHIRPS (Climate Hazards Group InfraRed Precipitation with Station data) [15–23]. However, satellite products are prone to systematic mistakes and biases, which may impair their accuracy [24,25]. To overcome this, many bias correction methods such as linear and nonlinear regression methods, quantile mapping, and machine learning techniques such as neural networks have been developed [26–35].

The basic goal of statistical bias correction techniques is to establish a statistical link between the variables being modeled and the observed data over the same historical time, and then to use that relationship to project the model [36]. For example, the quantile-based mapping approach aims to project the cumulative distribution function (CDF) of the model outputs into the distribution of the observations. This strategy can enhance not only the mean but the complete distribution of the variables [37–39]. Another bias correction technique is the Artificial neural networks (ANNs), which is are powerful nonlinear regression algorithms that capable of approximating practically any continuous input and output mapping [40,41]. ANN model is more practical than other standard modeling methods because to its processing speed and capacity to handle complicated nonlinear systems [42]. The ANN's robust, fault-tolerant, and parallel structure, which makes ANN models a potent and resilient instruments for global climate models and ecological research[43]. For instance, Maier et al. [44] reviewed more than 200 journal publications from 1999 to 2007 that used ANN models to predict flow in rivers.

The quality satellite rainfall products have been evaluated in some regions in Saudi Arabia. For example, Almazroui et al. [45] evaluated rainfall data for Saudi Arabia collected by the Tropical Rainfall Measuring Mission (TRMM) between 1998 and 2009. Although the TRMM product showed varying degrees of accuracy, Almazroui et al. [45] suggest that TRMM can be used to make up for the absence of rain gauges. Tekeli [46] had favorable results while using TRMM-3B42RT to identify an extraordinary precipitation occurrence in Jeddah, Saudi Arabia. Tekeli and Fouli [47] proposed an early flood warning system for Riyadh using the TRMM rainfall product for flash flood forecasting and came to the conclusion that during such a severe occurrence, the TRMM product might give some useful information. The three IMERG products were verified by Mahmoud et al. [48] over Saudi Arabia using ground rainfall measurements at daily and event time periods. They recommended adopting the IMERG Final version as an additional or alternative source of precipitation data for locations that have inadequate or nonexistent readings. AL-Areeq et al. [49] compared the performance of the three satellite rainfall products: IMERG, TRMM, and PERSIANN-CCS, across a 1725 km^2 arid watershed over Makkah watershed. The study suggested that IMERG's Early and late products are more reliable for predicting rainfall and its hydrological effects in arid areas.

The motivation of this study is to improve the accuracy of precipitation estimates in the region and to provide more reliable information for various applications, including water resource management, agriculture, and disaster management. The specific of this study include the following: a) comparison of the accuracy of multi-satellite-based precipitation estimates with ground-based measurements in Makkah region; b) evaluation of the effectiveness of bias correction methods, such as statistical methods, and machine learning methods, in correcting the systematic errors or biases in satellite-based estimates of precipitation in the study area; c) provide recommendations for the selection of bias correction methods based on the characteristics of the datasets and the specific application in Makkah. The findings of the study can significantly enhance water resources management in Saudi Arabia. Considering the limited number of rainfall monitoring stations available in the study area, satellite data can be a valuable source of information. Once corrected, it can offer a comprehensive view of rainfall patterns across the study area, especially in the sparsely populated eastern part of the Makkah region. By analyzing long-term satellite data records, decision-makers can obtain insights into rainfall trends and climate variability over time. This information can prove to be invaluable in making informed decisions.

The current work is structured as follows: Section 2 provides an overview of the materials and procedures used in the study. The evaluations' outcomes are shown in Section 3, while the discussion is presented in Section 4. Conclusions are finally presented in Section 5.

1. Material and Methods

1.1 Study Area

Makkah region is considered the one of the most important regions in Saudi Arabia because of its historical and religious significance, high population density, economic significance as the commercial hub, and placement at the center of the western region's middle section. The Red Sea, Riyadh Province, Al-Madinah Al-Munawwarah, and the provinces of Al Baha and Asir form the western, eastern, northern, and southern limits of Makkah's administrative boundaries (Fig. 1). Makkah's 141,216 km^2 administrative area is located between 18° 15′ and 23° 50′ N latitude and 38° 42′ to 43° 47′ E longitude. From 1966 to 2010, yearly rainfall over Makkah City ranged from 3.8 to 318.5 mm, with an annual average of 102.6 mm [50].

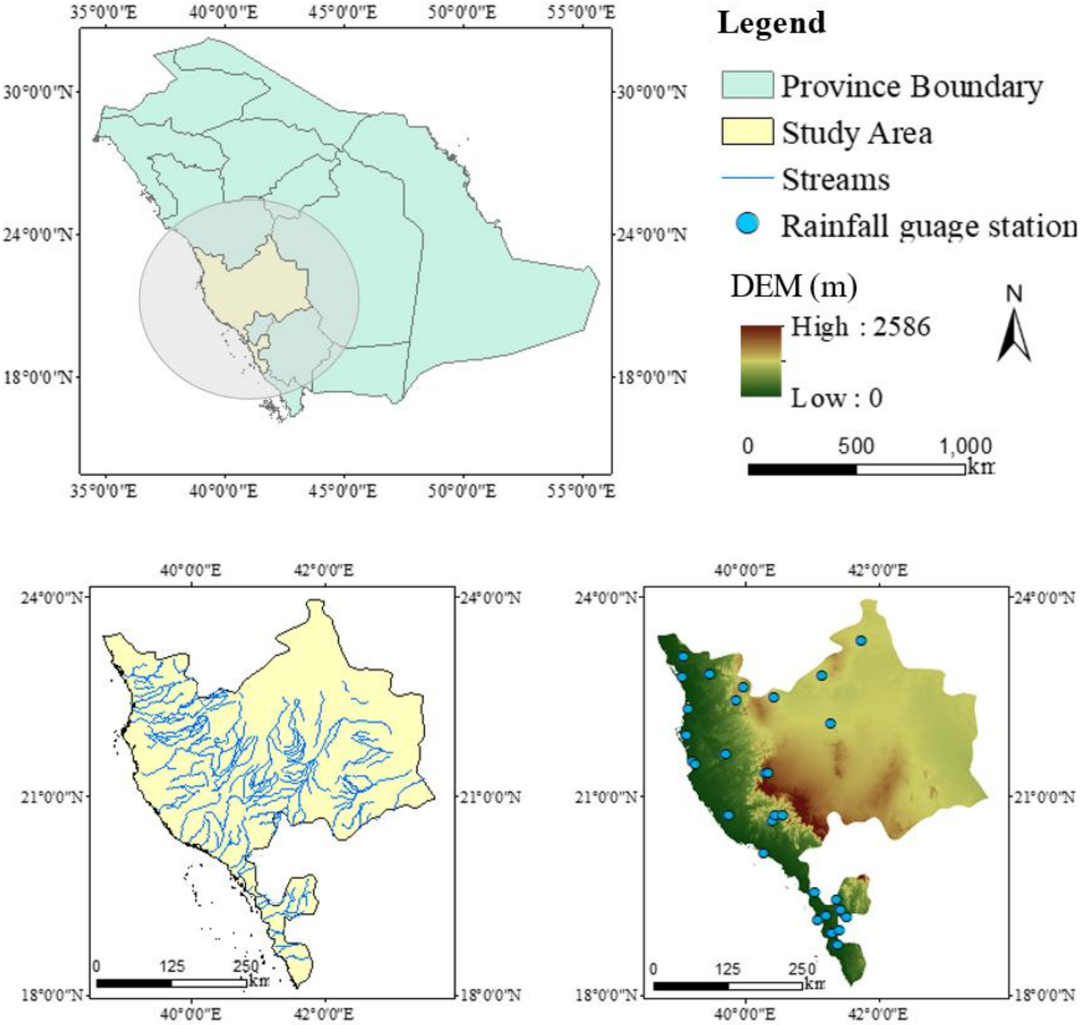

Figure 1: The study area

1.2 Ground Rain Gauge Data

Surface meteorological stations provide daily observation data, which is acquired from the Ministry of Environment, Water, and Agriculture. This research used daily precipitation data from January 2015 to November 2020 collected from 28 stations to verify the accuracy of the Satellite precipitation product. The quality of precipitation data was assessed for outliers, normality, homogeneity, and bias using four statistical tests: Kolmogorov-Smirnov, Shapiro-Wilk, Lilliefors, and Breusch-Pagan.

1.3 Satellite Products

The key features of the five satellite-based precipitation products (SBPs) employed in this study are shown in Table 1. The SBPs were obtained from their respective host websites, which are both free and open source. CHIRPS, PERSIANN, CDR, GPCP, and GPM are the five SBPs under consideration. CHIRPS was created principally by the USGS Famine Early Warning Systems Network and the University of California's Climate Hazards Group [51]. With a high spatial accuracy of 0.05 from 50S to 50N, it has supplied precipitation products worldwide since 1981. The CHIRPS has attracted a lot of attention and found a lot of uses recently because to its long recording periods and excellent spatial resolution [52,53].

The University of California, Irvine's Center for Hydrometeorology and Remote Sensing developed PERSIANN [21]. PERSIANN calculates the precipitation rate using cloud-top temperature inferred from IR pictures [54]. PERSIANN CDR, with a three-month time lag, is a long-term (from 1983 to the present) daily calibrated product with a reasonably high spatial resolution (0.25) that is commonly used for trend analyses of hydrometeorological events. In this work, PERSIANN CDR (hereinafter referred to as PERSIANN) was used for the comparison analysis.

The GPCP monthly precipitation dataset is a collaborative analysis of global rainfall patterns spanning from 1979 to the present. Data from multiple sources are merged on a worldwide 2.5° 2.5° grid, including microwave-based estimates from the Special Sensor Microwave Imager (SSM/I), rainfall estimations derived from surface rain gauges, infrared (IR) observations made by geostationary and polar-orbiting satellites. The analytic approach is intended to capitalize on the unique capabilities of the distinct input datasets, particularly in terms of bias reduction [55].

GPM was created by NASA in partnership with JAXA as the successor to NASA's TMPA and is another extensively used precipitation product of the GPM mission generated with the IMERG algorithm[56]. The extensive and uninterrupted historical data of the retroactive IMERG precipitation product enhances its usefulness in the field of hydrometeorology research and practical applications. The IMERG Final Run, which has been calibrated using data from the Global Precipitation Climatology Centre (GPCC) rain gauges, provides more accurate estimates and has been used for comparison in this study.

Table 1. Summary of satellite-related precipitation products used in this study

Data set	Resolution	coverage	Finest temporal resolution	Period
CHIRPS	0.05°× 0.05°	50° N – 50° S	Daily	1981- present
PERSIANN	0.25°× 0.25°	60 S-60 N	Daily	1983-present
CDR	0.25°× 0.25°	60 S-60 N	Daily	1983-present
GPCP	2.5°× 2.5°	Global	Monthly	1979-present
GPM	0.1 °× 0.1°	60 S- 60 N	Daily	2000-present

1.4 Precipitation Correction Methods

1.4.1 Linear correction method

In the linear correction approach, the daily precipitation quantities (P) obtained from the satellite are adjusted using a transformation equation, resulting in a transformed variable (P*). This transformation equation is given by

$$P^{*} = aP \qquad (1)$$

where (a) represents the scaling factor. The scaling factor (a) is determined by the ratio of the monthly mean observed precipitation ($\bar{O}$) to the monthly mean precipitation from the satellite ($\bar{P}$).

The linear correction approach is classified within the same category as the 'factor of change' or 'delta change' method, as discussed by Hay et al. [57]. The present approach possesses the benefit of being straightforward and requiring a little amount of data. Specifically, it needs just monthly climatological data in order to compute monthly correction factors. Nevertheless, focusing solely on adjusting the average monthly precipitation might potentially skew the comparative fluctuation of the distribution of precipitation across months and may have negative consequences on other statistical measures of daily precipitation probability distribution [58].

1.4.2 Nonlinear correction method

The authors of [59,60] advocate using power-law adjustments since a linear scaling factor will change the mean of the monthly precipitation but will not change the standard deviation of the precipitation.

$$P^{*} = aP^{b} \qquad (2)$$

where b is a scaling exponent.

It has an advantage with the linear technique in that it calls for monthly observed data, but it also requires knowledge of the coefficient of variation of precipitation (CV) in addition to the mean. While the nonlinear approach does not directly address biases in higher-order moments, it does mitigate them to some extent

2.4.3 Quantile Mapping

Additional bias correction strategies that are more flexible also aim to modify the variance of the model distribution in order to align it more accurately with the observed variance [61]. Quantile mapping is a generalized technique that encompasses all of these techniques. It involves the use of a quantile-based modification of distributions[62].

The widely used nonparametric quantile mapping technique involves aligning the empirical cumulative distribution function (CDF) of satellite-derived precipitation estimates with those of gauge measurements by the use of a transfer function. The procedure for computing the empirical cumulative distribution functions (CDFs) is described by Wilks[63] and used for the quantile mapping (QM) of daily precipitation data from climate models by Themeßl et al. [64].

2.4.4 Artificial Neural Network (ANN)

An artificial neural network (ANN) methodology is used to acquire knowledge of the bias structure by analyzing historical model outputs and their related observations [36]. The capacity of artificial neural networks (ANNs) to generalize is enhanced by including diverse forms of information and using a sufficiently big network to prevent overfitting to the specific stored knowledge and experiences. The architecture of the artificial neural network (ANN) is derived on the organization of biological brain systems, with numerous layers of artificial neurons (also known as nodes). The input layer is composed of input nodes that are linked to the input variables. The hidden layers, which may be one or more, are also connected to the input nodes. The output layer consists of output nodes that provide the output variables.

To determine the bias-corrected precipitation from the Satellite precipitation using ANN, a direct mapping is performed using the Satellite precipitation as the input and the observed precipitation as the output.

The objective is to optimize the performance and decrease the Root Mean Square Error (RMSE) of the corrected precipitation, while also assuring a tighter alignment with the standard deviation and mean of the measured precipitation. The optimal output was obtained using a three-layer feed-forward network with 35 hidden nodes. Out of a total of 214 data points for monthly precipitation, 150 (70%) are allocated for training, 32 (15%) for testing, and the remaining 32 for verification (15%).

The determination of the number of hidden layers often involves a trial-and-error approach [65]. The best number of hidden layers in this research was 35 as a result of trial and error.

Figure 2 depicts the arrangement of a feedforward three-layer artificial neural network (ANN). These types of artificial neural networks (ANNs) have a broad range of applications, including data storage and retrieval, pattern classification, input-output mapping, pattern grouping, and solving limited optimization problems.

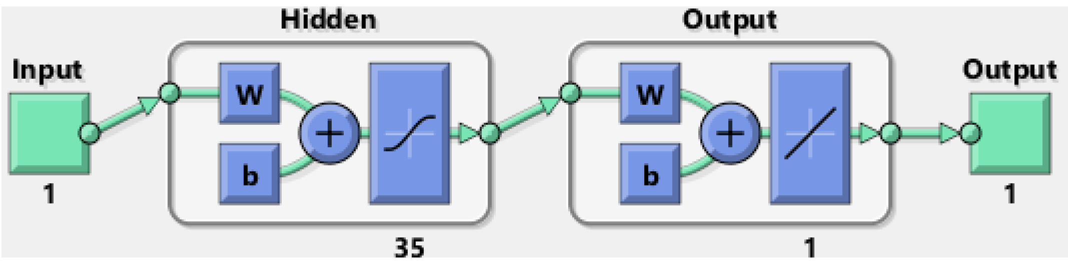

Figure 2 Setting up a Feedforward Three-Layer ANN Configuration for bias Correction

1.5 Statistical Evaluation

The performance of the satellite products was evaluated by comparing it with the monthly rainfall data obtained from each rain gauge. The rainfall data for the same latitude and longitude was collected from both the satellite and the rain gauge and then integrated into a monthly scale. After that, a comparison was made using four statistical metrics - Correlation Coefficient (CC), Relative Bias (RB), Mean Absolute Error (MAE), and Root Mean Square Error (RMSE). The CC indicates the level of agreement between the satellite estimation and the rain gauge observation regarding dynamics. The RB measures the systematic bias of satellite rainfall from rain gauge observations. The MAE provides the magnitude of inaccuracy, while the RMSE calculates the average absolute error of satellite rainfall. Smaller values of RMSE suggest more agreement between the two datasets.

Table 3: Statistical metrics for evaluating SBP

Statistical Metrics	Formula	Optimal Value
Root Mean Square Error (RMSE)	$RMSE = \sqrt{\frac{1}{n}\sum_{i=1}^{n}(x_i - y_i)^2}$	0
correlation coefficient (CC)	$CC = \frac{\sum_{i=1}^{n}(x_i - \overline{x})\,(y_i - \overline{y})}{\sqrt{\sum_{i=1}^{n}(x_i - \overline{x})^2 \sum_{i=1}^{n}(y_i - \overline{y})^2}}$	1
Relative bias (RB)	$RB = \frac{\sum_{i=1}^{n}(x_i - y_i)}{\sum_{i=1}^{n} y_i} * 100$	0
Mean Absolute Error (MAE)	$MAE = \frac{\sum_{i=1}^{n} \lvert y_i - x_i \rvert}{n}$	0

Note: y_i denotes gauged rainfall; x_i denotes satellite rainfall; n denotes the number of samples in the rainfall data pair time series; $\bar{y}$ and $\bar{x}$ denote the mean of the gauge and satellite rainfall datasets, respectively.

2. Results

2.1 Evaluation of precipitation products at the monthly scale

The geographical distribution of the annual average rainfall, as determined using observed data and SBPs, is shown in Figure 2. The IDW approach was employed to interpolate all the SBPs to assess their effectiveness in reproducing the geographical distribution of rainfall. For IDW interpolation, a pairwise comparison was performed with the rain gauge locations as the reference. The rainfall from each satellite product was obtained at the 28 locations, and then IDW interpolation was performed. Figure 2 shows the actual and predicted rainfall distribution for the Makkah region. The research area included both low rainfall regions in the northeast coastal region and high rainfall zones in the middle part of Makkah. The PERSIANN dataset tends to overestimate precipitation levels over the whole study area, with particularly pronounced overestimation in the western region. Conversely, the GPM dataset indicated considerably greater rainfall in the northern portion of the Makkah region.

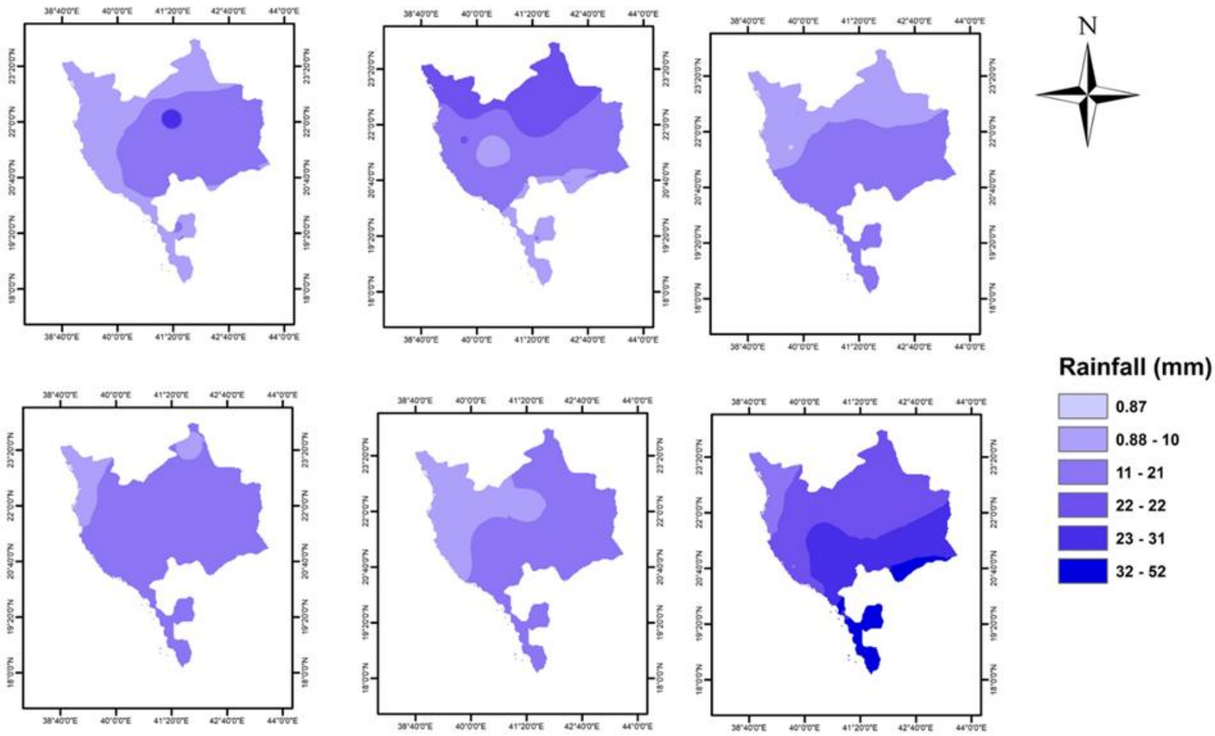

*Figure. 2 Annual average rainfall estimated using (**a**) observed data, (**b**) GPM, (**c**) GPCP, (d) PERSIANN -CDR,(e) CHIRPS, and (**f**) PERSIANN.*

Comparisons were performed using scatterplots of monthly precipitation from all precipitation products and the rain gauge data over the study area. Figure 3 shows the best and worst performers among the precipitation products. Overall, the GPM product showed the highest level of accuracy, while the PERSIANN product showed the weakest performance in terms of RMSE, CC, RB, and MAE values. To enhance the overall performance of IR-based algorithms, it is recommended that rainfall estimates be corrected with data from rain gauges at different elevations[66] . Given that the GPM product was the only one to be better in all statistical criteria, bias correction methods will only be applied to GPM, as will be discussed in the following section.

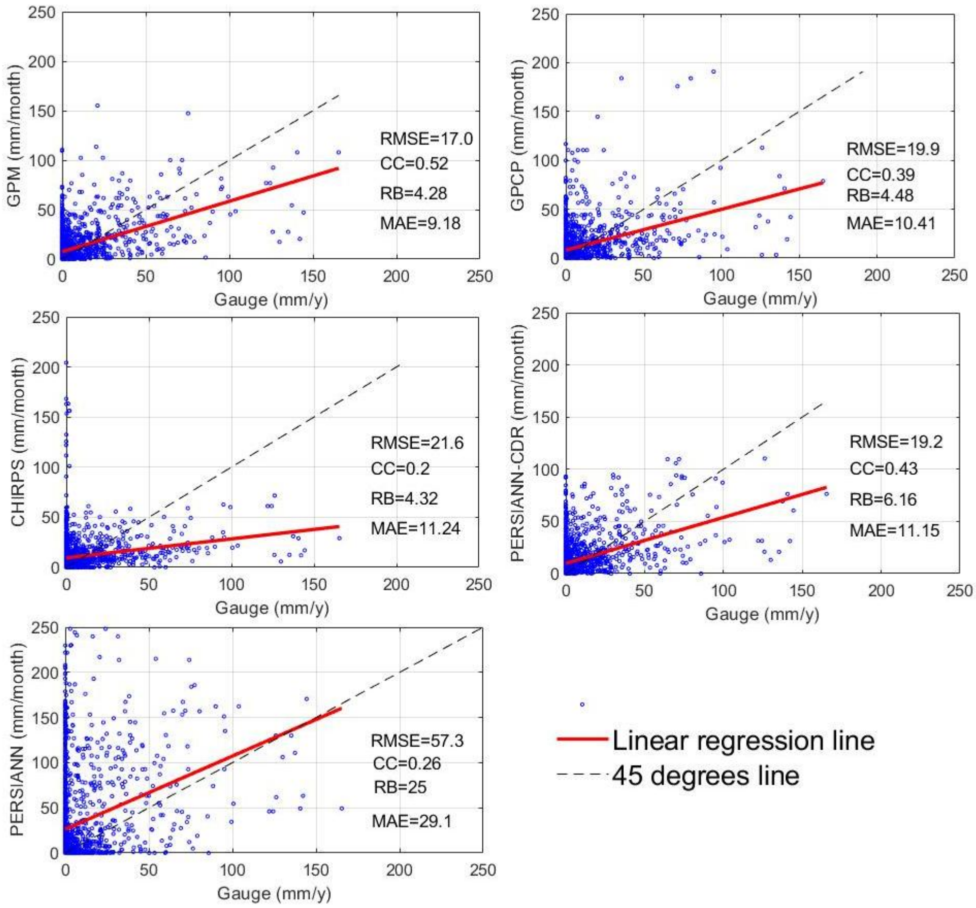

Figure. 3 Scatterplots of monthly precipitation from all gridded products against the observed rain gauge data over the study area. Angle between 45° (dashed) line and the regression (continuous) line is representative of the bias between series.

2.2 Evaluation of Bias correction methods

Figure 4 presents four scatter plots of different correction methods (linear, nonlinear, QM, and ANN) compared to observed data. The x-axis represents the gauge observed data (mm), and the y-axis represents GPM corrected data (mm). The red regression lines indicate the fitted models, while the 45-degree line is used as a reference. The results show that the linear method clusters data points around lower gauge values, while the nonlinear method has more spread in data points. The QM method has a wider spread of data points, while the ANN method shows a uniform distribution across gauge values. The ANN method shows the best results, with an RMSE of 13.75, CC of 0.59, RB of 0.025 and a MAE of 6.89.

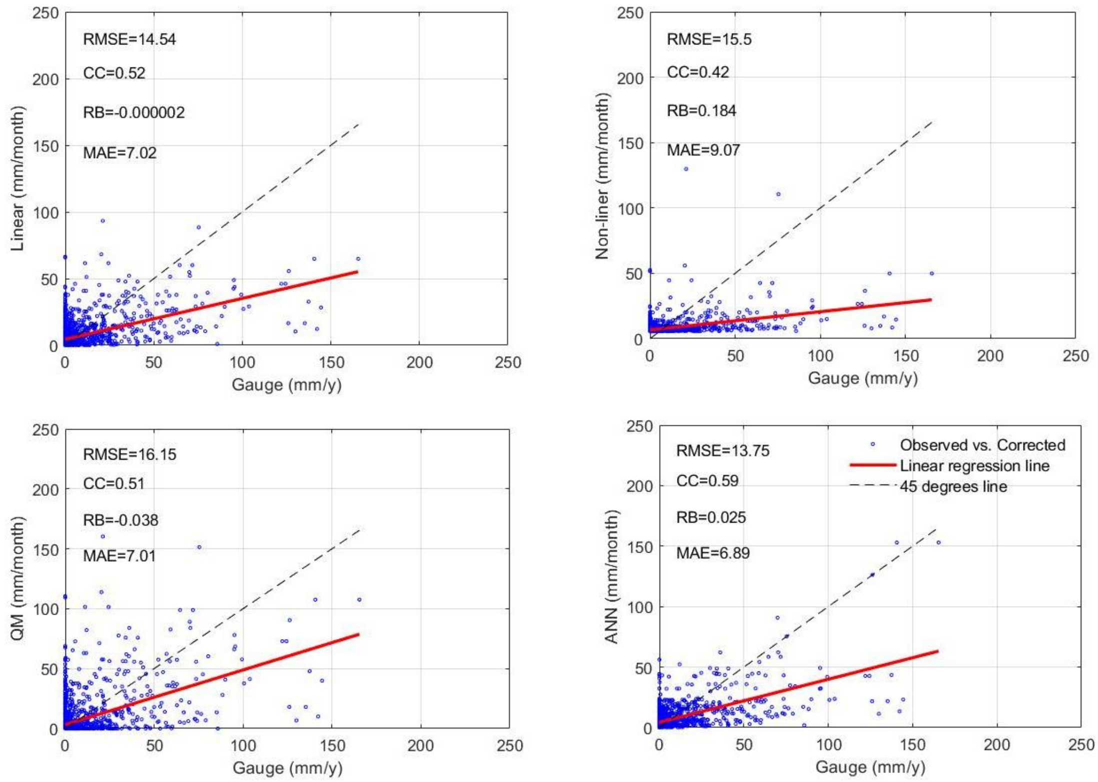

Figure 5 Scatter plots of different correction methods (linear, nonlinear, QM, and ANN) compared to observed data

3. Discussion

The focus is on evaluating and contrasting many satellite-based precipitation products (SBPs) for the Makkah region. We performed a comparative study of the rainfall time series at six sites from 2015 to 2020 to evaluate the performance of the SBPs. Four statistical indicators were used for assessment, and the results were shown in Figure 3. The results show that GPM had the lowest median Root Mean Square Error (RMSE) value among the SBPs, indicating it performed the best. PERSIANN, on the other hand, had the largest RMSE value, indicating worse accuracy in replicating actual rainfall. The GPM also demonstrated a robust association with the observed station data, as seen by its higher correlation coefficient (CC) value in comparison to other SBPs.

Overall, our findings showed that satellite products significantly overestimated Rainfall. Previous studies on Satellites showed that products often overestimate rainfall in arid regions due to various factors [67]. One factor is the limited ground-based rain gauge networks in the study regions which lead to sparse data coverage, making it challenging to estimate precipitation. Additionally, the topographical complexity of the study area, such as mountainous terrain, can further contribute to inaccuracies in satellite-based rainfall estimates[68–70]. Therefore, Bias correction techniques, such as ANN, are crucial in improving the performance of satellite products by adjusting for these overestimations.

Furthermore, the frequency and intensity of rainfall events in the study area differ from those in more temperate areas, leading to discrepancies in estimating rainfall amounts. A combination of data limitations, terrain complexities, and regional climatic characteristics contributed to the tendency of rainfall satellite products to overestimate precipitation in the study regions.

The findings show that, based on the compilation of average monthly observed and satellite rainfall data from 2015 to 2020, the GPM has a superior match in comparison to other SBPs. PERSIANN-CDR showed good performance following GPM, however, PERSIANN had the lowest accuracy in representing the observed rainfall probability. The research indicates that GPM is the most dependable SBP for rainfall estimation in the Makkah area because to its persistent reduced errors, greater correlation with observed data, and superior fit to the observed rainfall distribution. The results underscore the significance of choosing suitable SBPs for precise rainfall evaluation and point out the constraints of specific datasets in this specific area.

4. Conclusion

This research assessed the accuracy of five SBP approaches (GPM, GPCP, CHIRPS, PERSIANN-CDR, and PERSIANN) in recreating observed monthly rainfall at 28 locations in western Saudi Arabia. Calculating the RMSE, CC, RB, and MAE allows for a more accurate representation of the disparity between the data collected from satellite-based precipitation (SBPs) and the data collected from observations. The results show that the GPM has the best performance, with a CC of 0.27 and an RMSE of 17 mm, while the CDR comes in second with a CC of 0.19 and an RMSE of 19.2 mm. On the other hand, the CHIRPS has the second-worst performance, with an RMSE of 21.6 mm and a CC of 0.04. The PERSIANN has its worst performance, with an RMSE of 57.3 mm and a CC of 0.07. In terms of performance, GPCP is somewhat in the middle, with a CC of 0.15 and an RMSE of 19.9 mm.

For bias correction, several correction algorithms may be used, including linear, nonlinear, QM, and ANN. The findings indicate that the linear technique tends to group data points closer to lower gauge values, while the nonlinear method exhibits more dispersion across data points. The QM technique exhibits a greater dispersion of data points, but the ANN method demonstrates a consistent distribution across gauge values. The ANN technique demonstrates excellent performance, achieving a RMSE of 13.75, a CC of 0.59, a RB of 0.025, and a MAE of 6.89.

Artificial neural network (ANN) machine learning approaches were shown to be more successful than classic bias correction methods such as linear scaling, nonlinear, and quantile mapping methods. The results indicate that the GPM product is a reliable instrument for precisely recording rainfall patterns in the research region.

As shown in this research and several others, satellite products indicate bias. Therefore, while there have been advancements in technology to provide accurate precipitation data, more study is needed to improve bias correction approaches and prioritize the use of machine learning technologies. Our next research target is envisioned like this.

Author Contributions: "Conceptualization, I.H.E., A.Q.K., A.O.A and R.S.A; methodology, I.H.E., A.Q.K., A.O.A and R.S.A; validation, I.H.E., A.Q.K. and A.O.A.; formal analysis, I.H.E., A.Q.K., A.O.A and R.S.A; data curation, I.H.E., A.Q.K., A.O.A and R.S.A; writing—original draft preparation, I.H.E., A.Q.K. and A.O.A.; writing—review and editing, I.H.E., A.Q.K. and A.O.A.; visualization, I.H.E., A.Q.K. and A.O.A. All authors have read and agreed to the published version of the manuscript."

Conflicts of Interest: The authors declare no conflicts of interest.

References

1. Tan, X.; Yong, B.; Ren, L. Error Features of the Hourly GSMaP Multi-Satellite Precipitation Estimates over Nine Major Basins of China. *Hydrology Research* **2017**, *49*, 761–779, doi:10.2166/nh.2017.263.
2. Kucera, P.A.; Ebert, E.E.; Turk, F.J.; Levizzani, V.; Kirschbaum, D.; Tapiador, F.J.; Loew, A.; Borsche, M. Precipitation from Space: Advancing Earth System Science. *Bulletin of the American Meteorological Society* **2013**, *94*, 365–375, doi:10.1175/BAMS-D-11-00171.1.
3. Dibi-Anoh, P.A.; Koné, M.; Gerdener, H.; Kusche, J.; N'Da, C.K. Hydrometeorological Extreme Events in West Africa: Droughts. *Surv Geophys* **2023**, *44*, 173–195, doi:10.1007/s10712-022-09748-7.
4. Ghodichore, N.; Dhanya, C.T.; Hendricks Franssen, H.-J. Isolating the Effects of Land Use Land Cover Change and Inter-Decadal Climate Variations on the Water and Energy Cycles over India, 1981–2010. *Journal of Hydrology* **2022**, *612*, 128267, doi:10.1016/j.jhydrol.2022.128267.
5. Mei, Y.; Anagnostou, E.N.; Nikolopoulos, E.I.; Borga, M. Error Analysis of Satellite Precipitation Products in Mountainous Basins. *Journal of Hydrometeorology* **2014**, *15*, 1778–1793, doi:10.1175/JHM-D-13-0194.1.
6. Tang, G.; Clark, M.P.; Papalexiou, S.M.; Ma, Z.; Hong, Y. Have Satellite Precipitation Products Improved over Last Two Decades? A Comprehensive Comparison of GPM IMERG with Nine Satellite and Reanalysis Datasets. *Remote Sensing of Environment* **2020**, *240*, 111697, doi:10.1016/j.rse.2020.111697.
7. Atiah, W.A.; Johnson, R.; Muthoni, F.K.; Mengistu, G.T.; Amekudzi, L.K.; Kwabena, O.; Kizito, F. Bias Correction and Spatial Disaggregation of Satellite-Based Data for the Detection of Rainfall Seasonality Indices. *Heliyon* **2023**, *9*, e17604, doi:10.1016/j.heliyon.2023.e17604.
8. Degefu, M.A.; Bewket, W.; Amha, Y. Evaluating Performance of 20 Global and Quasi-Global Precipitation Products in Representing Drought Events in Ethiopia I: Visual and Correlation Analysis. *Weather and Climate Extremes* **2022**, *35*, 100416, doi:10.1016/j.wace.2022.100416.
9. Xie, P.; Janowiak, J.E.; Arkin, P.A.; Adler, R.; Gruber, A.; Ferraro, R.; Huffman, G.J.; Curtis, S. GPCP Pentad Precipitation Analyses: An Experimental Dataset Based on Gauge Observations and Satellite Estimates. *Journal of Climate* **2003**, *16*, 2197–2214, doi:10.1175/2769.1.
10. Xie, P.; Xiong, A.-Y. A Conceptual Model for Constructing High-Resolution Gauge-Satellite Merged Precipitation Analyses. *Journal of Geophysical Research: Atmospheres* **2011**, *116*, doi:10.1029/2011JD016118.
11. Bouizrou, I.; Bouadila, A.; Aqnouy, M.; Gourfi, A. Assessment of Remotely Sensed Precipitation Products for Climatic and Hydrological Studies in Arid to Semi-Arid Data-Scarce Region, Central-Western Morocco. *Remote Sensing Applications: Society and Environment* **2023**, *30*, 100976, doi:10.1016/j.rsase.2023.100976.

12. Saddique, N.; Muzammil, M.; Jahangir, I.; Sarwar, A.; Ahmed, E.; Aslam, R.A.; Bernhofer, C. Hydrological Evaluation of 14 Satellite-Based, Gauge-Based and Reanalysis Precipitation Products in a Data-Scarce Mountainous Catchment. *Hydrological Sciences Journal* **2022**, *67*, 436–450, doi:10.1080/02626667.2021.2022152.
13. Sun, Q.; Miao, C.; Duan, Q.; Ashouri, H.; Sorooshian, S.; Hsu, K.-L. A Review of Global Precipitation Data Sets: Data Sources, Estimation, and Intercomparisons. *Reviews of Geophysics* **2018**, *56*, 79–107, doi:10.1002/2017RG000574.
14. Shaowei, N.; Jie, W.; Juliang, J.; Xiaoyan, X.; Yuliang, Z.; Fan, S.; Linlin, Z. Comprehensive Evaluation of Satellite-Derived Precipitation Products Considering Spatial Distribution Difference of Daily Precipitation over Eastern China. *Journal of Hydrology: Regional Studies* **2022**, *44*, 101242, doi:10.1016/j.ejrh.2022.101242.
15. Duarte, L.V.; Formiga, K.T.M.; Costa, V.A.F. Analysis of the IMERG-GPM Precipitation Product Analysis in Brazilian Midwestern Basins Considering Different Time and Spatial Scales. *Water* **2022**, *14*, 2472, doi:10.3390/w14162472.
16. Zhou, L.; Koike, T.; Takeuchi, K.; Rasmy, M.; Onuma, K.; Ito, H.; Selvarajah, H.; Liu, L.; Li, X.; Ao, T. A Study on Availability of Ground Observations and Its Impacts on Bias Correction of Satellite Precipitation Products and Hydrologic Simulation Efficiency. *Journal of Hydrology* **2022**, *610*, 127595, doi:10.1016/j.jhydrol.2022.127595.
17. Lu, X.; Chen, Y.; Tang, G.; Wang, X.; Liu, Y.; Wei, M. Quantitative Estimation of Hourly Precipitation in the Tianshan Mountains Based on Area-to-Point Kriging Downscaling and Satellite-Gauge Data Merging. *J. Mt. Sci.* **2022**, *19*, 58–72, doi:10.1007/s11629-021-6901-5.
18. Guo, B.; Xu, T.; Yang, Q.; Zhang, J.; Dai, Z.; Deng, Y.; Zou, J. Multiple Spatial and Temporal Scales Evaluation of Eight Satellite Precipitation Products in a Mountainous Catchment of South China. *Remote Sensing* **2023**, *15*, 1373, doi:10.3390/rs15051373.
19. Reddy, N.M.; Saravanan, S. Evaluation of the Accuracy of Seven Gridded Satellite Precipitation Products over the Godavari River Basin, India. *Int. J. Environ. Sci. Technol.* **2023**, *20*, 10179–10204, doi:10.1007/s13762-022-04524-x.
20. Huffman, G.J.; Adler, R.F.; Morrissey, M.M.; Bolvin, D.T.; Curtis, S.; Joyce, R.; McGavock, B.; Susskind, J. Global Precipitation at One-Degree Daily Resolution from Multisatellite Observations. *Journal of Hydrometeorology* **2001**, *2*, 36–50, doi:10.1175/1525-7541(2001)002<0036:GPAODD>2.0.CO;2.
21. Ashouri, H.; Hsu, K.-L.; Sorooshian, S.; Braithwaite, D.K.; Knapp, K.R.; Cecil, L.D.; Nelson, B.R.; Prat, O.P. PERSIANN-CDR: Daily Precipitation Climate Data Record from Multisatellite Observations for Hydrological and Climate Studies. *Bulletin of the American Meteorological Society* **2015**, *96*, 69–83, doi:10.1175/BAMS-D-13-00068.1.
22. Salmani-Dehaghi, N.; Samani, N. Development of Bias-Correction PERSIANN-CDR Models for the Simulation and Completion of Precipitation Time Series. *Atmospheric Environment* **2021**, *246*, 117981, doi:10.1016/j.atmosenv.2020.117981.
23. Funk, C.; Peterson, P.; Landsfeld, M.; Pedreros, D.; Verdin, J.; Shukla, S.; Husak, G.; Rowland, J.; Harrison, L.; Hoell, A.; et al. The Climate Hazards Infrared Precipitation with Stations—a New Environmental Record for Monitoring Extremes. *Sci Data* **2015**, *2*, 150066, doi:10.1038/sdata.2015.66.
24. Li, W.; Jiang, Q.; He, X.; Sun, H.; Sun, W.; Scaioni, M.; Chen, S.; Li, X.; Gao, J.; Hong, Y. Effective Multi-Satellite Precipitation Fusion Procedure Conditioned by Gauge Background Fields over the Chinese Mainland. *Journal of Hydrology* **2022**, *610*, 127783, doi:10.1016/j.jhydrol.2022.127783.
25. Atiah, W.A.; Johnson, R.; Muthoni, F.K.; Mengistu, G.T.; Amekudzi, L.K.; Kwabena, O.; Kizito, F. Bias Correction and Spatial Disaggregation of Satellite-Based Data for the Detection of Rainfall Seasonality Indices. *Heliyon* **2023**, *9*, e17604, doi:10.1016/j.heliyon.2023.e17604.

26. Zhang, L.; Chen, X.; Lai, R.; Zhu, Z. Performance of Satellite-Based and Reanalysis Precipitation Products under Multi-Temporal Scales and Extreme Weather in Mainland China. *Journal of Hydrology* **2022**, *605*, 127389, doi:10.1016/j.jhydrol.2021.127389.
27. Sun, Z.; Long, D.; Hong, Z.; Hamouda, M.A.; Mohamed, M.M.; Wang, J. How China's Fengyun Satellite Precipitation Product Compares with Other Mainstream Satellite Precipitation Products. *Journal of Hydrometeorology* **2022**, *23*, 785–806, doi:10.1175/JHM-D-21-0179.1.
28. Peña-Guerrero, M.D.; Umirbekov, A.; Tarasova, L.; Müller, D. Comparing the Performance of High-Resolution Global Precipitation Products across Topographic and Climatic Gradients of Central Asia. *International Journal of Climatology* **2022**, *42*, 5554–5569, doi:10.1002/joc.7548.
29. Dangol, S.; Talchabhadel, R.; Pandey, V.P. Performance Evaluation and Bias Correction of Gridded Precipitation Products over Arun River Basin in Nepal for Hydrological Applications. *Theor Appl Climatol* **2022**, *148*, 1353–1372, doi:10.1007/s00704-022-04001-y.
30. Ageet, S.; Fink, A.H.; Maranan, M.; Diem, J.E.; Hartter, J.; Ssali, A.L.; Ayabagabo, P. Validation of Satellite Rainfall Estimates over Equatorial East Africa. *Journal of Hydrometeorology* **2022**, *23*, 129–151, doi:10.1175/JHM-D-21-0145.1.
31. Nwachukwu, P.N.; Satge, F.; Yacoubi, S.E.; Pinel, S.; Bonnet, M.-P. From TRMM to GPM: How Reliable Are Satellite-Based Precipitation Data across Nigeria? *Remote Sensing* **2020**, *12*, 3964, doi:10.3390/rs12233964.
32. Satgé, F.; Defrance, D.; Sultan, B.; Bonnet, M.-P.; Seyler, F.; Rouché, N.; Pierron, F.; Paturel, J.-E. Evaluation of 23 Gridded Precipitation Datasets across West Africa. *Journal of Hydrology* **2020**, *581*, 124412, doi:10.1016/j.jhydrol.2019.124412.
33. Wu, Z.; Xu, Z.; Wang, F.; He, H.; Zhou, J.; Wu, X.; Liu, Z. Hydrologic Evaluation of Multi-Source Satellite Precipitation Products for the Upper Huaihe River Basin, China. *Remote Sensing* **2018**, *10*, 840, doi:10.3390/rs10060840.
34. Seo, G.-Y.; Ahn, J.-B. Comparison of Bias Correction Methods for Summertime Daily Rainfall in South Korea Using Quantile Mapping and Machine Learning Model. *Atmosphere* **2023**, *14*, 1057, doi:10.3390/atmos14071057.
35. Salehnia, N.; Ahn, J. Modelling and Reconstructing Tree Ring Growth Index with Climate Variables through Artificial Intelligence and Statistical Methods. *Ecological Indicators* **2022**, *134*, 108496, doi:10.1016/j.ecolind.2021.108496.
36. Moghim, S.; Bras, R.L. Bias Correction of Climate Modeled Temperature and Precipitation Using Artificial Neural Networks. *Journal of Hydrometeorology* **2017**, *18*, 1867–1884, doi:10.1175/JHM-D-16-0247.1.
37. Hayhoe, K.; Cayan, D.; Field, C.B.; Frumhoff, P.C.; Maurer, E.P.; Miller, N.L.; Moser, S.C.; Schneider, S.H.; Cahill, K.N.; Cleland, E.E.; et al. Emissions Pathways, Climate Change, and Impacts on California. *Proceedings of the National Academy of Sciences* **2004**, *101*, 12422–12427, doi:10.1073/pnas.0404500101.
38. Cayan, D.R.; Maurer, E.P.; Dettinger, M.D.; Tyree, M.; Hayhoe, K. Climate Change Scenarios for the California Region. *Climatic Change* **2008**, *87*, 21–42, doi:10.1007/s10584-007-9377-6.
39. Maurer, E.P.; Hidalgo, H.G. Utility of Daily vs. Monthly Large-Scale Climate Data: An Intercomparison of Two Statistical Downscaling Methods. *Hydrology and Earth System Sciences* **2008**, *12*, 551–563, doi:10.5194/hess-12-551-2008.
40. Hornik, K. Approximation Capabilities of Multilayer Feedforward Networks. *Neural Networks* **1991**, *4*, 251–257, doi:10.1016/0893-6080(91)90009-T.
41. Hornik, K.; Stinchcombe, M.; White, H. Multilayer Feedforward Networks Are Universal Approximators. *Neural Networks* **1989**, *2*, 359–366, doi:10.1016/0893-6080(89)90020-8.

42. Moghim, S.; Bras, R.L. Bias Correction of Climate Modeled Temperature and Precipitation Using Artificial Neural Networks. *Journal of Hydrometeorology* **2017**, *18*, 1867–1884, doi:10.1175/JHM-D-16-0247.1.
43. Liu, Z.; Peng, C.; Xiang, W.; Tian, D.; Deng, X.; Zhao, M. Application of Artificial Neural Networks in Global Climate Change and Ecological Research: An Overview. *Chin. Sci. Bull.* **2010**, *55*, 3853–3863, doi:10.1007/s11434-010-4183-3.
44. Maier, H.R.; Jain, A.; Dandy, G.C.; Sudheer, K.P. Methods Used for the Development of Neural Networks for the Prediction of Water Resource Variables in River Systems: Current Status and Future Directions. *Environmental Modelling & Software* **2010**, *25*, 891–909, doi:10.1016/j.envsoft.2010.02.003.
45. Almazroui, M.; Islam, M.N.; Jones, P.D.; Athar, H.; Rahman, M.A. Recent Climate Change in the Arabian Peninsula: Seasonal Rainfall and Temperature Climatology of Saudi Arabia for 1979–2009. *Atmospheric Research* **2012**, *111*, 29–45, doi:10.1016/j.atmosres.2012.02.013.
46. Tekeli, A.E. Exploring Jeddah Floods by Tropical Rainfall Measuring Mission Analysis. *Water* **2017**, *9*, 612, doi:10.3390/w9080612.
47. Tekeli, A.E.; Fouli, H. Evaluation of TRMM Satellite-Based Precipitation Indexes for Flood Forecasting over Riyadh City, Saudi Arabia. *Journal of Hydrology* **2016**, *541*, 471–479, doi:10.1016/j.jhydrol.2016.01.014.
48. Mahmoud, M.T.; Al-Zahrani, M.A.; Sharif, H.O. Assessment of Global Precipitation Measurement Satellite Products over Saudi Arabia. *Journal of Hydrology* **2018**, *559*, 1–12, doi:10.1016/j.jhydrol.2018.02.015.
49. Al-Areeq, A.M.; Al-Zahrani, M.A.; Sharif, H.O. Assessment of the Performance of Satellite Rainfall Products over Makkah Watershed Using a Physically Based Hydrologic Model. *Appl Water Sci* **2022**, *12*, 246, doi:10.1007/s13201-022-01768-3.
50. Dawod, G.M.; Mirza, M.N.; Al-Ghamdi, K.A. Assessment of Several Flood Estimation Methodologies in Makkah Metropolitan Area, Saudi Arabia. *Arab J Geosci* **2013**, *6*, 985–993, doi:10.1007/s12517-011-0405-5.
51. Funk, C.; Peterson, P.; Landsfeld, M.; Pedreros, D.; Verdin, J.; Shukla, S.; Husak, G.; Rowland, J.; Harrison, L.; Hoell, A.; et al. The Climate Hazards Infrared Precipitation with Stations—a New Environmental Record for Monitoring Extremes. *Sci Data* **2015**, *2*, 150066, doi:10.1038/sdata.2015.66.
52. Aksu, H.; Akgül, M.A. Performance Evaluation of CHIRPS Satellite Precipitation Estimates over Turkey. *Theor Appl Climatol* **2020**, *142*, 71–84, doi:10.1007/s00704-020-03301-5.
53. Nicholson, S.E.; Klotter, D.A. Assessing the Reliability of Satellite and Reanalysis Estimates of Rainfall in Equatorial Africa. *Remote Sensing* **2021**, *13*, 3609, doi:10.3390/rs13183609.
54. Nguyen, P.; Ombadi, M.; Sorooshian, S.; Hsu, K.; AghaKouchak, A.; Braithwaite, D.; Ashouri, H.; Thorstensen, A.R. The PERSIANN Family of Global Satellite Precipitation Data: A Review and Evaluation of Products. *Hydrology and Earth System Sciences* **2018**, *22*, 5801–5816, doi:10.5194/hess-22-5801-2018.
55. Gu, G.; Adler, R.F.; Huffman, G.J.; Curtis, S. Tropical Rainfall Variability on Interannual-to-Interdecadal and Longer Time Scales Derived from the GPCP Monthly Product. *Journal of Climate* **2007**, *20*, 4033–4046, doi:10.1175/JCLI4227.1.
56. Huffman, G.J.; Bolvin, D.T.; Braithwaite, D.; Hsu, K.; Joyce, R.; Kidd, C.; Nelkin, E.J.; Sorooshian, S.; Tan, J.; Xie, P. NASA Global Precipitation Measurement (GPM) Integrated Multi-Satellite Retrievals for GPM (IMERG). Algorithm Theoretical Basis Document (ATBD) Version 06. *NASA/GSFC* **2019**, *30*.
57. Hay, L.E.; Clark, M.P.; Wilby, R.L.; Gutowski, W.J.; Leavesley, G.H.; Pan, Z.; Arritt, R.W.; Takle, E.S. Use of Regional Climate Model Output for Hydrologic Simulations. *Journal of Hydrometeorology* **2002**, *3*, 571–590, doi:10.1175/1525-7541(2002)003<0571:UORCMO>2.0.CO;2.

58. Diaz-Nieto, J.; Wilby, R.L. A Comparison of Statistical Downscaling and Climate Change Factor Methods: Impacts on Low Flows in the River Thames, United Kingdom. *Climatic Change* **2005**, *69*, 245–268, doi:10.1007/s10584-005-1157-6.
59. Shabalova, M.V.; Deursen, W.P.A. van; Buishand, T.A. Assessing Future Discharge of the River Rhine Using Regional Climate Model Integrations and a Hydrological Model. *Climate Research* **2003**, *23*, 233–246, doi:10.3354/cr023233.
60. Leander, R.; Buishand, T.A. Resampling of Regional Climate Model Output for the Simulation of Extreme River Flows. *Journal of Hydrology* **2007**, *332*, 487–496, doi:10.1016/j.jhydrol.2006.08.006.
61. Teutschbein, C.; Seibert, J. Bias Correction of Regional Climate Model Simulations for Hydrological Climate-Change Impact Studies: Review and Evaluation of Different Methods. *Journal of Hydrology* **2012**, *456–457*, 12–29, doi:10.1016/j.jhydrol.2012.05.052.
62. Maraun, D. Bias Correcting Climate Change Simulations - a Critical Review. *Curr Clim Change Rep* **2016**, *2*, 211–220, doi:10.1007/s40641-016-0050-x.
63. Wilks, D. *Statistical Methods in the Atmospheric Sciences*; Academic Press: Cambridge: USA, 2011; Vol. 100; ISBN 0-12-385022-3.
64. Themeßl, M.J.; Gobiet, A.; Heinrich, G. Empirical-Statistical Downscaling and Error Correction of Regional Climate Models and Its Impact on the Climate Change Signal. *Climatic Change* **2012**, *112*, 449–468, doi:10.1007/s10584-011-0224-4.
65. ASCE Task Committee on Application of Artificial Neural Networks in Hydrology Artificial Neural Networks in Hydrology. II: Hydrologic Applications. *J. Hydrol. Eng.* **2000**, *5*, 124–137, doi:10.1061/(ASCE)1084-0699(2000)5:2(124).
66. Thorne, V.; Coakeley, P.; Grimes, D.; Dugdale, G. Comparison of TAMSAT and CPC Rainfall Estimates with Raingauges, for Southern Africa. *International Journal of Remote Sensing* **2001**, *22*, 1951–1974, doi:10.1080/01431160118816.
67. Zeng, W.; Ding, X.; Sun, W.; Mu, X. Improvement of Satellite-Based Rainfall Product CHIRPS in Estimating Rainfall Erosivity on the Loess Plateau. *Land Degradation & Development* **2023**, *34*, 4517–4528, doi:10.1002/ldr.4790.
68. Rachidi, S.; El Mazoudi, E.H.; El Alami, J.; Jadoud, M.; Er-Raki, S. Assessment and Comparison of Satellite-Based Rainfall Products: Validation by Hydrological Modeling Using ANN in a Semi-Arid Zone. *Water* **2023**, *15*, 1997, doi:10.3390/w15111997.
69. Baig, F.; Abrar, M.; Chen, H.; Sherif, M. Evaluation of Precipitation Estimates from Remote Sensing and Artificial Neural Network Based Products (PERSIANN) Family in an Arid Region. *Remote Sensing* **2023**, *15*, 1078, doi:10.3390/rs15041078.
70. Macharia, D.; Fankhauser, K.; Selker, J.S.; Neff, J.C.; Thomas, E.A. Validation and Intercomparison of Satellite-Based Rainfall Products over Africa with TAHMO In Situ Rainfall Observations. *Journal of Hydrometeorology* **2022**, *23*, 1131–1154, doi:10.1175/JHM-D-21-0161.1.